Linking Interfacial Plasticity to Ductility: A Modeling Framework for Nanostructured Metals

Ting Zhu[1], Ju Li[2], Amit Samanta[2], Hyoung Gyu Kim[2] and Subra Suresh[3]

[1] *Woodruff School of Mechanical Engineering, Georgia Institute of Technology, Atlanta, Georgia 30332, USA*

[2] *Department of Materials Science and Engineering, Ohio State University, Columbus, Ohio 43210, USA and*

[3] *Department of Materials Science and Engineering, Massachusetts Institute of Technology, Cambridge, Massachusetts 02139, USA**

(Dated: September 8, 2006)

Nano-twinned copper exhibits an unusual combination of ultrahigh strength and high ductility, along with increased strain-rate sensitivity. We develop a mechanistic framework for predicting the rate sensitivity and elucidating the origin of ductility in terms of the interactions of dislocations with interfaces. Using atomistic reaction pathway calculations, we show that twin boundary (TB) mediated slip transfer reactions are the rate-controlling mechanisms of plastic flow. We attribute the relatively high ductility of nano-twinned copper to the hardenability of TBs as they gradually lose coherency during deformation. These results offer new avenues for tailoring material interfaces for optimized properties.

Nanocrystalline metals with grain size finer than 100nm routinely exhibit up to five times higher strength than their coarse-grained counterparts, but suffer from greatly diminished ductility[1,2,3]. Experiments show that introduction of coherent nano-twins, typically tens of nm in thickness, in ultrafine grained copper (with grain size of several hundred nms) leads to an unusual combination of ultrahigh strength (about 1GPa) and high ductility (14% elongation to failure)[4,5,6]. The plastic deformation characteristics of nanocrystalline metals have previously been rationalized on the basis of a number of mechanisms[7], including grain boundary (GB) sliding[8,9], grain rotation[10], and diffusional creep[11]. An effective experimental technique to probe the active deformation mechanism is to measure the sensitivity of flow stress to the rate of loading[34], because both the sensitivity index m and the associated activation volume $v^\star$ can vary by orders of magnitude for different rate-limiting processes. For face-centered cubic metals such as copper, grain refinement into the nanocrystalline regime leads to an increase in m by up to an order of magnitude relative to microcrystalline metals, and a concomitant decrease in the activation volume $v^\star$ by two orders of magnitude[12,13]. Nano-twinned copper shows the same characteristics of increased rate sensitivity and reduced activation volume as nanocrystalline copper without twins[4,5,14]; the puzzle is that it does not achieve very high strength by severely compromising ductility[6].

The prevailing model for nanocrystals is the Hall-Petch relation[7,15], which is a scaling function relating strength to grain size. The Hall-Petch relation is derived based on strengthening mechanisms[16] at internal interfaces, which proliferate in nanocrystals. However, it says nothing about ductility. To model ductility, we have to go back to the detailed physical processes at materials interfaces, in particular those involving carriers of plastic strain - dislocations. Dislocation mechanisms at internal interfaces usually involve slip transfer from one slip system to another mediated by the interface[9,17]. Consider a GB separating bulk crystals 1 and 2. The simplest slip transfer reactions are binary: the absorption of a bulk dislocation into GB to become a GB dislocation $\mathbf{b}_{\rm bulk1} \rightarrow \mathbf{b}_{\rm GB}$, or the reverse desorption reaction $\mathbf{b}_{\rm GB} \rightarrow \mathbf{b}_{\rm bulk2}$. But also common are ternary reactions such as $\mathbf{b}_{\rm bulk1} \rightarrow \mathbf{b}_{\rm bulk2} + \mathbf{b}_{\rm GB}$ or $\mathbf{b}_{\rm GB1} \rightarrow \mathbf{b}_{\rm GB2} + \mathbf{b}_{\rm bulk}$.

Here we model prototypical slip transfer reactions, both binary and ternary, near $\Sigma 3$ $\{111\}$ TB (a singular GB) by atomistic reaction path calculations[18,19]. The technique we use, climbing image nudged elastic band (CINEB) method[20], is a chain-of-states atomistic approach[18,19,21] that does not suffer from the severe strain-rate limitations associated with

molecular dynamics simulations. It has been shown to be extremely valuable for the quantification of thermally activated rate processes[18,19], i.e., the atomistically calculated activation energy and activation volume can be directly compared with laboratory experiments performed at seconds-and-hours timescale. We have made an important improvement to the original CINEB method by allowing a movable end state as detailed in Methods. By this improvement the computational efficiency is significantly enhanced for an accurate characterization of the saddle-point configurations of dislocation reactions.

Consider a $\langle 1\bar{1}0\rangle$ screw dislocation shown in Fig. 1a,b, initially in the upper half of the bicrystal (bulk 1), subjected to an anti-plane shear stress that drives it towards the TB. Given a prescribed shear strain γ, we first obtain the relaxed atomic configuration using single-point energy minimization. With $\gamma = 0.02$, the leading Shockley partial dislocation is held up right at the TB, followed by the trailing Shockley partial $\sim 4b$ behind. The far-field resolved shear stress (RSS) is $\tau = 252\,\mathrm{MPa} \approx 0.006G$, where $G = 42\,\mathrm{GPa}$ is the $\{111\}\langle 1\bar{1}0\rangle$ shear modulus. We also find from single-point calculations that when τ is greater than the athermal threshold stress for transmission $\tau^{\mathrm{ath}}_{\mathrm{tms}} = 340\,\mathrm{MPa}$, the dislocation transmits across the TB into bulk 2 without the aid of thermal activation. This is in accord with experimentally measured yield strength $\sigma \sim 1$GPa of nano-twinned copper, since there is a conversion ratio $M \approx 3.1$ (Taylor factor) between the macroscopic tensile stress σ in a polycrystal and the RSS on a slip system[22]. The calculated athermal threshold stress for absorption is very close to 340 MPa as well.

We probe the kinetic pathways of slip transfer reaction using the CINEB method when the applied shear stress is below the athermal threshold. Two competing pathways are identified as illustrated in Fig. 1b, with the corresponding atomic configurations shown in Fig. 1c. The first path is a two-step process involving the absorption of the incoming screw dislocation into the TB, followed by desorption. Due to the special geometry, there is no residual Burgers vector content left in the TB after the two steps. We find that both absorption and desorption occur by the "Friedel-Escaig" type cross-slip mechanism, where the two partials first constrict to a full screw dislocation, and then spread into TB (absorption) or bulk 2 (desorption). In contrast, the second pathway involves direct transmission of the incoming screw dislocation by the "Fleischer" type cross-slip, where the leading partial penetrates into bulk 2 without waiting for the trailing partial still yet in bulk 1. This process temporarily leaves a sessile stair-rod dislocation on the TB, which is only freed when the trailing partial

catches up. Thus the TB acts as a sink or source of dislocations, as well as a barrier against direct transmission.

According to transition state theory, the rate of slip transfer reaction is given by $\nu \exp(-Q/k_{\rm B}T)$, where ν is the attempt frequency, Q is the activation energy, $k_{\rm B}$ is Boltzmann's constant, and T the temperature. We have computed the activation energy Q associated with each saddle point. At $\tau = 252\,{\rm MPa}$, the CINEB calculation gives $Q_{\rm abs} = 0.49\,{\rm eV}$ (absorption), and $Q_{\rm tms} = 0.67\,{\rm eV}$ (direct transmission), respectively. By contrast, $Q_{\rm des}$ is much higher for desorption, with a value of $\sim 5\,{\rm eV}$. The large value of $Q_{\rm des}$ arises because clean TBs are very deep traps for Shockley dislocations. Unlike when they are in the bulk, Shockley partials in TB are unbounded by stacking fault because their Burgers vectors coincide with the displacement shift complete (DSC) lattice of the TB. With imposed periodic boundary conditions on the simulation supercell, the two partials would separate to exactly one-half of the supercell width to minimize the elastic energy, whereas in reality they would separate to infinity on an infinite, clean TB (and simultaneously, the TB would migrate by one atomic spacing in $\langle 111 \rangle$). Thus a large activation energy is needed to constrict the two widely separated TB Shockley partials during desorption.

In order to show that TB-mediated slip transfer reactions are indeed the rate-controlling steps of plastic flow, we then compute the true activation volume, $\Omega \equiv -\partial Q/\partial\tau$, which can be taken as a kinetic signature of deformation mechanism[23]. We find $\Omega_{\rm tms} \approx 79b^3$ at $\tau = 252\,{\rm MPa}$. Similarly, we calculate $\Omega_{\rm ads} \approx \Omega_{\rm des} \approx 43b^3$ for absorption and desorption. These true activation volumes from atomistic calculations compare favorably with the experimentally measured apparent activation volume $v^\star \equiv \sqrt{3}k_{\rm B}T\partial \ln\dot{\epsilon}/\partial\sigma$ of $\sim 10 - 20b^3$ for nano-twinned copper[14]. Here $\dot{\epsilon}$ denotes the tensile strain rate; there is a conversion factor $\sqrt{3}/M$ relating Ω to $v^\star$. To summarize, our atomistic calculation predicts the following macroscopic properties: $\sigma = M\tau = 780\,{\rm MPa}$, $v^\star = \Omega\sqrt{3}/M = 24 - 44b^3$, $m = \sqrt{3}k_{\rm B}T/v^\star\sigma = 0.013 - 0.023$, at a laboratory strain rate corresponding to $Q \approx 0.49 - 0.67{\rm eV}$. This parameter-free prediction is for an idealized situation where the TB is perfect without pre-existing dislocations, $\rho_{\rm int} = 0$, and the twin lamellae are thin enough ($\sim 10\,{\rm nm}$) that only a single bulk dislocation can pile up at the TB. To our knowledge, this is the first atomistic calculation that predicts reasonable strain-rate dependence of flow stress which can be directly compared with laboratory experiments (Table 1). Also shown for contrast in Table 1 are results from classical theories based on diffusion-controlled processes and bulk

forest hardening. They are clearly excluded as possible mechanisms.

The kinetic rates of slip transfer reactions will dynamically evolve with dislocation content in the twin boundary. Specifically, assuming the same attempt frequency ν for different reactions, a lower $Q_{\rm abs}$ gives a higher kinetic rate of absorption compared to that of desorption. An imbalance in the rates of absorption and desorption will cause accumulation of interfacial dislocations (see Fig. 2). The accumulated TB dislocations will in turn affect the activation energies due to dislocation-dislocation interactions. According to Le Chatelier's principle, this should be expected to suppress subsequent absorption, enhance desorption and change the direct transmission rates, such that a quasi-steady state of reactions is eventually reached at the TB.

We coarse-grain over time the above atomic-scale processes to establish an absorption-desorption-transmission (ADT) kinetic equation, shown in Fig. 2, where $\rho_{\rm int}$ denotes the density of TB dislocations, defined as the total length of dislocations per unit TB area. $J_{\rm tms}$ is the dislocation flux of direct transmission from bulk 1 to 2, $J_{\rm abs}$ from bulk 1 to TB, and $J_{\rm des}$ from TB to bulk 2. The ADT equation should generally serve as boundary condition for bulk dislocation density ($\rho_{\rm bulk}$) based crystal plasticity models[24]. However for nanocrystals, the role played by bulk crystal plasticity would be greatly reduced since dislocations seldom stay inside the bulk, but are either absorbed into or piled up near the GB. Correspondingly, the role of interfacial plasticity processes, as regulators of bulk dislocation fluxes and as carriers of plastic strain themselves, is markedly enhanced. In nano-twinned copper, the twin lamellae may be approximated as transparent (barrierless) to bulk dislocation flux if they are less than $\sim$ 10nm thick[4,14]. The main resistance to plastic flow comes from the TBs, which we have shown to provide a satisfactory estimate of the macroscopic yield stress.

The rate of transmission $J_{\rm tms}(\tau, \rho_{\rm int})$ is proportional to $\exp(-Q_{\rm tms}(\tau, \rho_{\rm int})/k_{\rm B}T)$ and similar forms hold for $J_{\rm abs}(\tau, \rho_{\rm int})$ and $J_{\rm des}(\tau, \rho_{\rm int})$. The sensitivity of $Q_{\rm tms}(\tau, \rho_{\rm int})$ and thus $J_{\rm tms}(\tau, \rho_{\rm int})$ to their first argument of shear stress τ is given by the activation volume, which we have discussed above. The sensitivity of $Q(\tau, \rho_{\rm int})$ to the second argument $\rho_{\rm int}$ turns out to be a critical quantity as well, and can be eventually related to the ductility. Here we first highlight the physical consequence of this dependence and then present calculations of $\rho_{\rm int}$ dependence of activation energy Q. We define the interfacial hardening rate as $\Pi \equiv -\partial J/\partial \rho_{\rm int}|_{\tau}$ that describes hardening of the TB as it becomes less coherent with more interfacial dislocations deposited in it. If it is agreed upon that the macroscopic yield stress

of a nanocrystal is dominated by interfacial resistance to dislocation motion - the essence of the Hall-Petch relation[7,9], then it should be plausible that the macroscopic strain hardening rate $\Theta \equiv \partial\sigma/\partial\epsilon|_{\dot{\epsilon}}$ (or the lack thereof[5]) reflects also, to a large degree, the interfacial hardening rate or the lack thereof. One thus expects a linear relationship between Θ and Π[35]. Θ is important because it directly governs the ductility of most nanocrystalline metals, which fail by severe plastic strain localization[5,25]. The higher the Π and therefore Θ, the better the ductility, and the larger the range of uniform elongation, because according to Considère's criterion, $\Theta < \sigma$ for the initiation of plastic strain localization[5,26].

Our atomistic calculations show that the activation barriers $Q(\tau, \rho_{\text{int}})$ of TB-meditated slip transfer reactions depend sensitively on ρ_{int}. By introducing an extra pair of Shockley dislocations in the TB, we find that Q_{tms} increases from 0.67eV to 1.3eV, at identical far-field stress $\tau = 252$MPa (see Fig. 3). Thus ρ_{int} dramatically influences $Q(\tau, \rho_{\text{int}})$. Generally we find that as ρ_{int} increases, both $Q_{\text{abs}}(\tau, \rho_{\text{int}})$ and $Q_{\text{tms}}(\tau, \rho_{\text{int}})$ increase, but $Q_{\text{des}}(\tau, \rho_{\text{int}})$ decreases.

The experimental condition is more complex, however. Instead of the present collinear dislocation geometry, a 2D interfacial dislocation network should be absorbed in the TB, in which case both ρ_{int} and the J-fluxes should be tensorial quantities[24] instead of scalars. However, we make the following general observation. Work hardening[23] in the bulk obeys the $\rho_{\text{bulk}}^{1/2}$-law which can be rationalized based on the scaling argument of a governing lengthscale L, the forest dislocation spacing $\propto \rho_{\text{bulk}}^{-1/2}$. The same scaling argument should be applicable to interfacial dislocation hardening[27]. Note that the governing lengthscale L is $\propto \rho_{\text{int}}^{-1}$ now because the interfacial dislocation networks are 2D as dislocations are trapped in the GBs and can only densify in-plane. Then we have an interfacial hardening law $\sigma = \sigma_0(d) + h(d)\mu b\rho_{\text{int}}$, where h is dimensionless and depends only on the grain size and μ denotes shear modulus of the polycrystal sample. Similar to bulk work hardening, as the governing lengthscale L (mesh spacing of interfacial dislocation network) refines, the material would harden, and the activation volume would decrease, compared to $\rho_{\text{int}} = 0$ values. Thus our σ and $v^\star$ predictions based on calculations at $\rho_{\text{int}} = 0$ seem to "err" on the right side compared to experiments.

The proposed hardening law $\sigma = \sigma_0(d) + h(d)\mu b\rho_{\text{int}}$ governing interfacial plasticity should work well for low-angle GBs, as well as GBs vicinal to special boundaries, when ρ_{int} ($\propto$ crystallographic ledge density on GB) is small. However, as ρ_{int} increases to a point where the

interfacial dislocation cores start to overlap, saturation must set in, similar to plateauing of the GB energy at large misorientation angle[28]. Then the GB hardening rate Π approaches zero. This explains the generally poor ductility of common nanocrystals produced by powder-consolidation or electrodeposition, as most of their GBs are high angle[25], so Π is small and therefore the grain assembly is susceptible to plastic strain localization. In contrast, nano-twinned copper has superior uniform elongation because TBs are singular interfaces[36], and are much more hardenable as they gradually lose coherency during deformation, which gives rise to an increased strain hardening rate and a consequent delay in the onset of necking[5] that leads to the improved tensile ductility.

In summary, the present modeling framework extends the timescale of atomistic simulations to provide both quantitative and mechanistic insights into the roles played by twin boundaries as nanostructural features that critically affect strength, rate sensitivity and ductility. The results help understand and point to possible routes for optimizing strong and ductile nanostructured metals through controlled introduction of coherent internal interfaces.

Movies of the minimum energy path of dislocation absorption, desorption and direct transmission at TB can be viewed at http://164.107.79.177/Stuff/tr/Movie/ (Supplementary Material).

Methods

The simulation cell consists of a symmetric bicrystal with a coherent $\Sigma 3$ $\{111\}$ TB in the middle. The cell size is 8.9nm $\times$ 11.8nm $\times$ 7.7nm (17.7nm $\times$ 11.8nm $\times$ 15.3nm), with a total of $N = 56\ 400$ (225 600) atoms; all the reported values are calculated using the large cell, although the small cell provides satisfactory energetics in most cases. Periodic boundary conditions are imposed in both the $\langle 112 \rangle$ and $\langle 110 \rangle$ directions, with free space above the top and below the bottom (111) surfaces. As shown in Fig. 1a, in the adjoining bicrystal a pair of symmetric (111) slip planes are inclined at $\theta = 70.5^\circ$ with respect to the twin plane, and they intersect along a common line in the TB. We probe slip transfer reactions between this particular pair of slip planes as well as between any one of them and the TB. We consider a straight dislocation that encounters the TB in screw orientation, i.e., the Burgers vector is parallel to the intersection of the slip plane and TB. This screw can cross-slip without leaving any residual content (e.g., stair-rod type dislocation) at the intersection of the slip plane in the TB. The interatomic interactions are modeled using the embedded-atom method (EAM) potential for Cu by Mishin et al.[29], which has been validated against *ab initio* calculations[30]. The stacking-fault energy given by the potential is 44.4mJ/m^2, close to the experimental measurement of 45mJ/m^2. The stress acting on the simulation cell is calculated using the Virial formula[30].

We quantify the TB mediated slip transfer reactions using atomistic reaction path calculations[18,19]. Under a given shear stress, the climbing image nudged elastic band (CINEB) method is employed to determine the minimum energy path (MEP) of reaction. The activation energy is given by the maximum on the MEP, a saddle point on the potential energy surface of the system. In a CINEB calculation, two end states are first determined, then a discretized elastic band consisting of a finite number of replicas (images) of the system is constructed by linear interpolation to connect the two states. With appropriate relaxation, the band converges to the MEP. In our calculations of dislocation-TB reactions, e.g. direct transmission, we choose an initial state where a screw dislocation in the upper crystal is fully relaxed and held up at the TB, and a final state where the dislocation has cross-slipped into the lower crystal but before reaching the fully relaxed state where it exits the crystal.

Free-end CINEB method: To relax the elastic band we have improved the original CINEB

method by allowing a movable end state while keeping its energy unchanged (it can only move on a $3N-1$ dimensional energy isosurface). This way, we can keep the end state close to the saddle-point/initial states in terms of the hyperspace path length. In our calculations the final-state energy is fixed at 0.1eV below the initial state, separated by the barrier. As a result, the number of replicas along the band can be significantly reduced, while retaining a reasonable density of replicas near the saddle point, e.g., 8 replicas are sufficient to obtain a converged saddle-point state that we have double-checked using the dimer method[31], a highly accurate approach for a local probe of the saddle point.

The true activation volume $\Omega \equiv -\partial Q/\partial\tau$ is related to the strain-rate sensitivity that one can measure experimentally. Physically Ω is proportional to the number of atoms that undergo coherent inelastic displacements at the saddle point. We can compute Ω by calculating two MEPs at slightly different stresses and then perform numerical differentiation, but there is also a second way based on perturbation theory that does not require two calculations, $\Omega = V \cdot (\tau_i - \tau_s)/G$, where V denotes the volume of bicrystal, G is the shear modulus in $\{111\}\langle 110\rangle$ direction, and τ_i, τ_s are the shear stress of the initial and saddle-point state, respectively, when the load is applied via displacement control.

---

* Electronic address: ting.zhu@me.gatech.edu, li.562@osu.edu, ssuresh@mit.edu

[1] Zhu, Y. T. T. & Liao, X. Z. Nanostructured metals - retaining ductility. *Nat. Mater.* **3**, 351–352 (2004).

[2] Jia, D. *et al.* Deformation behavior and plastic instabilities of ultrafine-grained titanium. *Appl. Phys. Lett.* **79**, 611–613 (2001).

[3] Koch, C. C. Optimization of strength and ductility in nanocrystalline and ultrafine grained metals. *Scr. Mater.* **49**, 657–662 (2003).

[4] Lu, L., Shen, Y. F., Chen, X. H., Qian, L. H. & Lu, K. Ultrahigh strength and high electrical conductivity in copper. *Science* **304**, 422–426 (2004).

[5] Ma, E. *et al.* Strain hardening and large tensile elongation in ultrahigh-strength nano-twinned copper. *Appl. Phys. Lett.* **85**, 4932–4934 (2004).

[6] Dao, M., Lu, L., Shen, Y. & Suresh, S. Strength, strain-rate sensitivity and ductility of copper with nano-scale twins. *Acta Mater.* in press (2006).

[7] Kumar, K. S., Van Swygenhoven, H. & Suresh, S. Mechanical behavior of nanocrystalline metals and alloys. *Acta Mater.* **51**, 5743–5774 (2003).

[8] Schiotz, J. & Jacobsen, K. W. A maximum in the strength of nanocrystalline copper. *Science* **301**, 1357–1359 (2003).

[9] Van Swygenhoven, H. Polycrystalline materials - grain boundaries and dislocations. *Science* **296**, 66–67 (2002).

[10] Shan, Z. W. *et al.* Grain boundary-mediated plasticity in nanocrystalline nickel. *Science* **305**, 654–657 (2004).

[11] Yamakov, V., Wolf, D., Phillpot, S. R., Mukherjee, A. K. & Gleiter, H. Deformation-mechanism map for nanocrystalline metals by molecular-dynamics simulation. *Nat. Mater.* **3**, 43–47 (2004).

[12] Schwaiger, R., Moser, B., Dao, M., Chollacoop, N. & Suresh, S. Some critical experiments on the strain-rate sensitivity of nanocrystalline nickel. *Acta Mater.* **51**, 5159–5172 (2003).

[13] Asaro, R. J. & Suresh, S. Mechanistic models for the activation volume and rate sensitivity in metals with nanocrystalline grains and nano-scale twins. *Acta Mater.* **53**, 3369–3382 (2005).

[14] Lu, L. *et al.* Nano-sized twins induce high rate sensitivity of flow stress in pure copper. *Acta Mater.* **53**, 2169–2179 (2005).

[15] Weertman, J. R. *et al.* Structure and mechanical behavior of bulk nanocrystalline materials. *MRS Bull.* **24**, 44–50 (1999).

[16] Li, J. C. M. Petch relation and grain boundary sources. *Trans Met Soc AIME* **227**, 239 (1963).

[17] Jin, Z. H. *et al.* The interaction mechanism of screw dislocations with coherent twin boundaries in different face-centred cubic metals. *Scr. Mater.* **54**, 1163–1168 (2006).

[18] Zhu, T., Li, J. & Yip, S. Atomistic study of dislocation loop emission from a crack tip. *Phys. Rev. Lett.* **93**, 025503 (2004).

[19] Zhu, T., Li, J. & Yip, S. Atomistic configurations and energetics of crack extension in silicon. *Phys. Rev. Lett.* **93**, 205504 (2004).

[20] Henkelman, G., Uberuaga, B. P. & Jonsson, H. A climbing image nudged elastic band method for finding saddle points and minimum energy paths. *J. Chem. Phys.* **113**, 9901–9904 (2000).

[21] Elber, R. & Karplus, M. A method for determining reaction paths in large molecules - application to myoglobin. *Chem. Phys. Lett.* **139**, 375–380 (1987).

[22] Taylor, G. I. Plastic strain in metals. *J. Inst. Metals* **62**, 307–324 (1938).

[23] Kocks, U. F., Argon, A. S. & Ashby, M. F. Thermodynamics and kinetics of slip. *Prog. Mater.*

Sci. **19**, 1–281 (1975).

[24] Arsenlis, A., Parks, D. M., Becker, R. & Bulatov, V. V. On the evolution of crystallographic dislocation density in non-homogeneously deforming crystals. *J. Mech. Phys. Solids* **52**, 1213–1246 (2004).

[25] Kumar, K. S., Suresh, S., Chisholm, M. F., Horton, J. A. & Wang, P. Deformation of electrodeposited nanocrystalline nickel. *Acta Mater.* **51**, 387–405 (2003).

[26] Wang, Y. M., Chen, M. W., Zhou, F. H. & Ma, E. High tensile ductility in a nanostructured metal. *Nature* **419**, 912–915 (2002).

[27] Hughes, D. A. & Hansen, N. Microstructure and strength of nickel at large strains. *Acta Mater.* **48**, 2985–3004 (2000).

[28] Sutton, A. P. & Balluffi, R. W. *Interfaces in crystalline materials* (Clarendon Press, Oxford, 1995).

[29] Mishin, Y., Mehl, M. J., Papaconstantopoulos, D. A., Voter, A. F. & Kress, J. D. Structural stability and lattice defects in copper: Ab initio, tight-binding, and embedded-atom calculations. *Phys. Rev. B* **6322**, 224106 (2001).

[30] Zhu, T. *et al.* Predictive modeling of nanoindentation-induced homogeneous dislocation nucleation in copper. *J. Mech. Phys. Solids* **52**, 691–724 (2004).

[31] Henkelman, G. & Jonsson, H. A dimer method for finding saddle points on high dimensional potential surfaces using only first derivatives. *J. Chem. Phys.* **111**, 7010–7022 (1999).

[32] Wang, Y. M. & Ma, E. Strain hardening, strain rate sensitivity, and ductility of nanostructured metals. *Mater. Sci. Eng. A* **375-77**, 46–52 (2004).

[33] Read, W. T. & Shockley, W. Dislocation models of crystal grain boundaries. *Phys. Rev.* **78**, 275–289 (1950).

[34] Consider a polycrystalline specimen under uniaxial tension, the empirical power-law relation between the stress σ and strain rate $\dot{\epsilon}$ is $\sigma/\sigma_0 = \left(\dot{\epsilon}/\dot{\epsilon}_0\right)^m$, where m is the non-dimensional rate sensitivity index. The apparent (tensile) activation volume $v^\star$ is customarily defined as $v^\star = \sqrt{3}k_{\rm B}T\partial \ln\dot{\epsilon}/\partial\sigma$. The sensitivity index m is then related to $v^\star$ by $m = \sqrt{3}k_{\rm B}T/(\sigma v^\star)$, both m and $v^\star$ provide quantitative measures of the sensitivity of flow stress to loading rate[14,32].

[35] Assuming the bulk is 100% transparent to dislocation flux, the system strain rate $\dot{\epsilon}$ is directly proportional to J: $\dot{\epsilon} = aJ$. Θ describes the necessary stress increase to maintain constant strain rate: $\Theta \equiv \partial\sigma/\partial\epsilon|_{\dot{\epsilon}}$, while Π describes the decrease in strain rate if the stress is hold constant. If

we assume $\rho_{\text{int}} = k\epsilon$, it can then be shown mathematically that $\Theta = k\Pi/\Omega$.

[36] These interfaces are called singular or special because they show up as cusps in the GB energy γ versus misorientation angle θ plot. Read and Shockley[33] derived the formula $\gamma \propto |\theta - \theta_0| \log |\theta - \theta_0|$, which has a singularity at the special misorientation $\theta = \theta_0$, indicating maximum sensitivity there. For small changes in θ from the special arrangement, there is $\rho_{\text{int}} \propto \theta - \theta_0$ and so $\gamma \propto \rho_{\text{int}} \log \rho_{\text{int}}$, which has a singularity at $\rho_{\text{int}} = 0$.

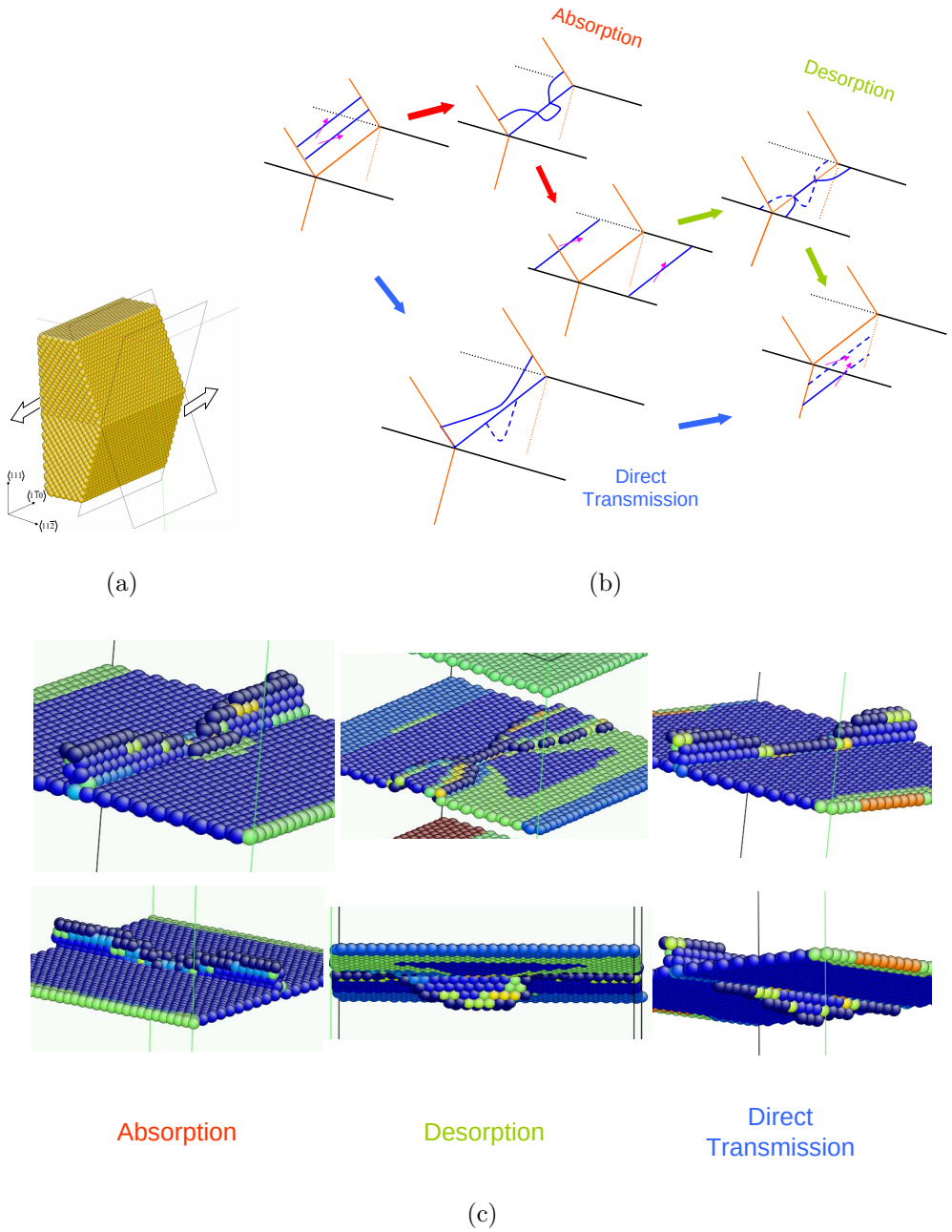

FIG. 1: (a) A symmetric bicrystal with a coherent $\Sigma 3$ {111} TB in the middle, subjected to anti-plane shear. The bicrystal is cut to expose a pair of symmetric (111) slip planes inclined at $\theta = 70.5°$ with respect to the TB. (b) Schematic of two competing pathways of slip-transfer reaction discovered from CINEB calculations. The first pathway is a two-step process involving the absorption of an incoming screw into the TB, followed by desorption. The second involves direct transmission of the screw across the TB. (c) Atomic configurations of absorption, desorption and direct transmission; two views are shown for each state. Atoms are color coded by the central symmetry parameter, showing the stacking fault and TB. Movies of these processes can be viewed in the Supplementary Material accompanying this paper.

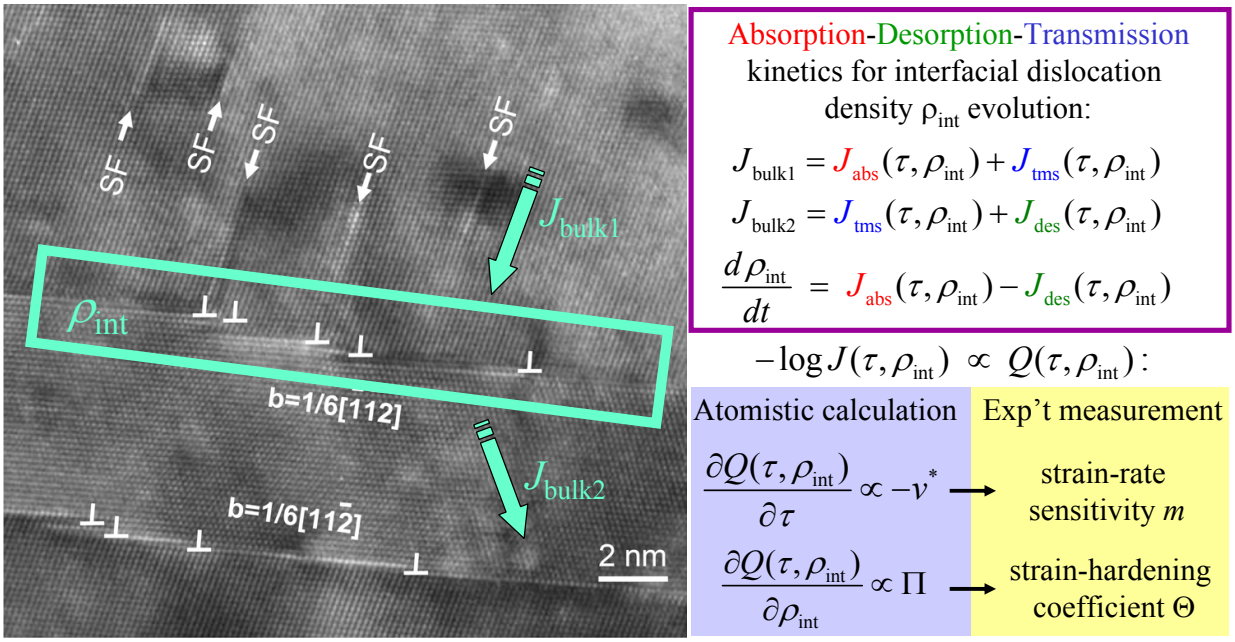

FIG. 2: Transmission Electron Microscopy image shows the accumulation of TB dislocations (from[6]); Coarse-graining the discrete atomic-scale processes over time establishes an absorption-desorption-transmission (ADT) kinetic equation.

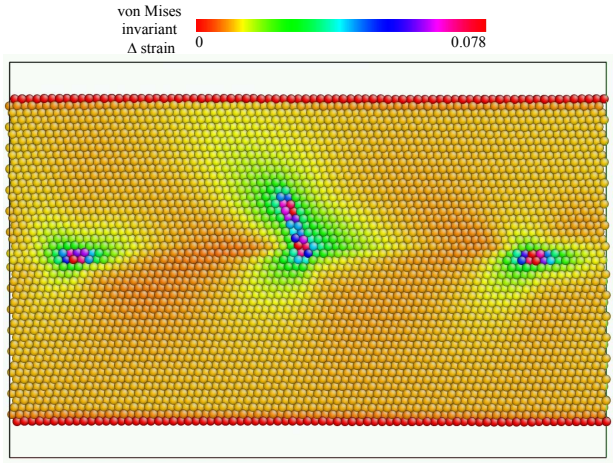

(a)

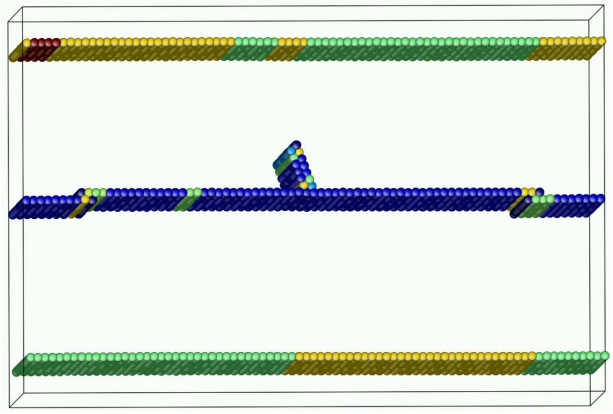

(b)

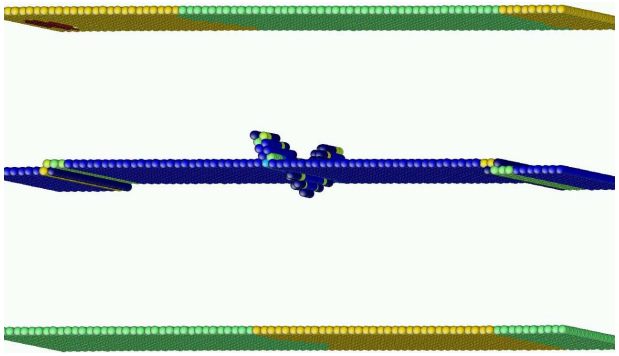

(c)

FIG. 3: Direct transmission under the influence of pre-existing TB dislocations. The pre-transmission equilibrium state is shown in (a) and (b); the transition state is shown in (c). Atoms are color coded by (a) Mises invariant of local strain (subtracting off the average strain), showing elastic interaction of the incoming screw with two TB Shockley partials, and (b),(c) the central symmetry parameter. Note the TB has migrated by one step after absorbing the two TB Shockley dislocations.

Table 1: Comparison of yield stress, activation volume and strain-rate sensitivity between experimental measurements and atomistic calculation

		yield stress	activation volume v^*	strain-rate sensitivity m
Nano-twinned Copper	Uniaxial tension [Lu04]	~1 GPa		
	Nanoindentation [Lu05]	> 700 MPa*	$12-22b^3$	$0.025-0.036$
	Atomistic calculation	780 MPa	$24-44b^3$	$0.013-0.023$
Diffusion-controlled processes			$\sim 0.1b^3$	~1
Bulk forest hardening		$\sim \mu b\sqrt{\rho_{\text{bulk}}}$	$100-1000b^3$	$0-0.005$

* extracted from measured hardness H as $\frac{H}{3}$.